

# Design and ground plane optimization of a CPW-fed ultra-wideband antenna

Mohammed AL-HUSSEINI<sup>1</sup>, Ali RAMADAN<sup>1</sup>, Youssef TAWK<sup>2</sup>, Ali EL-HAJJ<sup>1</sup>,  
Karim Y. KABALAN<sup>1</sup>

<sup>1</sup>Department of Electrical and Computer Engineering, American University of Beirut,  
Beirut, 1107 2020, LEBANON

e-mails: husseini@ieee.org, {ahr06, elhajj, kabalan}@aub.edu.lb

<sup>2</sup>Department of Electrical and Computer Engineering, University of New Mexico,  
Albuquerque, NM 87131, USA

e-mail: yatawk@ece.unm.edu

## Abstract

*In this paper, an ultra-wideband antenna based on an egg-shaped conductor and a co-planar waveguide (CPW) feed is presented. The ground plane incorporates an egg-shaped slot with parametrized center and dimensions. By resizing the slot and moving its center, a slotted or a partial ground can be obtained. Based on this configuration, a parametric study that aims at achieving the best ultra-wideband (UWB) response of the antenna is done. The study shows that an excellent UWB response is achieved for a certain ground slot size, beyond which the response starts to degrade. However, as the slot size tends to infinity, thus leading to a partial rectangular ground plane, the UWB property again emerges. A second parametric study is done to find the length of the partial rectangular ground plane that gives the best UWB profile.*

*As a result, two optimal designs are generated. Prototypes of the two are fabricated and their return loss is measured. Other characteristics are computed using a Finite-Element-based EM solver. The radiation patterns, peak gain, and radiation efficiency of both optimal configurations are presented and compared. The results show that the design with the slotted ground yields better omni-directional patterns and higher gains in the principal planes. The second design has slightly larger radiation efficiency and larger peak gains at high frequencies.*

**Key Words:** Printed antennas, UWB, CPW.

## 1. Introduction

In 2002, the Federal Communication Commission (FCC) declared the 3.1–10.6 GHz frequency band for use in commercial communication applications [1]. Since then, interest in ultra-wideband wireless communication has increased tremendously, and has led to extensive research effort aiming at innovating and developing new antennas for ultra-wideband operation.

Printed antennas have proved to be a good choice for these systems due to their low profile, small size, light weight, low cost, and ease of fabrication and integration in microwave circuits [2]. With co-planar waveguide (CPW) feeds, extra advantages are acquired, such as wider bandwidth, better impedance matching, lower radiation loss, and less dispersion [3, 4].

Several CPW-fed ultra-wideband antenna designs have been reported in the literature. These can differ, among other factors, by the shape of the conductor and the configuration of the ground plane. In [5], the presented CPW-fed ultra-wideband antenna is based on circular disc conductor, and a partial rectangular ground plane. The antenna in [6] features a step-typed monopole conductor with a step-slope ground plane. In [7], the antenna consists of an open annulus strip as a ground plane and an open crescent patch in the inner space of the annulus as a radiating element. The authors of [8] introduce annular slot and round corners into the ground and use a round-edged bowtie-shaped conductor. Four circular and elliptical ultra-wideband (UWB) antenna designs are presented in [9], where two of them are CPW-based and the other two are microstrip-line fed. The designs are also different in size, where the smallest is  $40 \times 35 \text{ mm}^2$ . The measured results in [10] show that a  $40 \times 38 \text{ mm}^2$  CPW-fed antenna with an elliptical slot has a bandwidth covering the range 3.1–10.6 GHz. This antenna is based on a U-shaped center conductor.

In this paper, a CPW-based antenna design for UWB operation is presented. The antenna is printed on a  $40 \times 30 \text{ mm}^2$  substrate. The center radiator has the shape of an egg, which is a combination of a circle and an ellipse. A parametric study shows that a specific size of the ground's egg-shaped slot results in an optimal UWB response. The UWB response re-appears for a partial rectangular ground plane, whose length is optimized using a second parametric study. The measured and computed results of the two optimal designs are reported and compared.

This paper is organized as follows. Section 2 describes the antenna configuration and the parameters under study. Section 3 presents the obtained results and discusses them. Finally, the conclusion is given in Section 4.

## 2. Antenna configuration

The configuration of the antenna is detailed in Figure 1. The substrate is  $3 \times 4 \text{ cm}^2$  in size, 1.6 mm in thickness, and is based on the FR4 epoxy material with dielectric constant  $\epsilon_r$  of 4.4. The  $50 \Omega$  feed line is 3 mm wide and 5 mm long. The egg-shaped center conductor is obtained by combining a circle and an ellipse. The circle has a radius of 9 mm, which is also the minor radius of the ellipse. The major radius of the ellipse (along the Y-axis) is 12.06 mm. The shape of the patch is well-suited to achieve larger bandwidths.

A slot, which has the shape of an egg and is formed the same way as the center conductor, is incorporated in the ground plane. The slot is parametrized, with  $R_g$  (in mm) being its smaller radius, and  $1.31 \times R_g$  being its larger radius.  $R_g$  is the radius of the circle and minor radius of the ellipse making the slot. The center of the slot is at  $R_g + 4.5$  mm from the edge of the feed. Increasing  $R_g$  changes the ground plane from slotted to partial, as shown in Figure 2. The first study involves varying the value of  $R_g$  to achieve the best UWB response.

The case  $R_g = \infty$  yields a partial ground plane that is rectangular in shape. For this configuration, which is shown in Figure 3, the length of the ground plane, denoted  $G_L$ , can also be optimized in search of a UWB response.

## 3. Results and discussion

All simulations were done using Ansoft HFSS [11], which is based on the Finite-Element Method (FEM). Figures 4 and 5 demonstrate the return loss of the antenna for several  $R_g$  values. For  $R_g = 14.5$  mm, a 2.2–12 GHz

impedance bandwidth is obtained. Beyond this  $R_g$  value, the UWB response deteriorates. The case  $R_g = 14.5$  mm is denoted Optimal Design I.

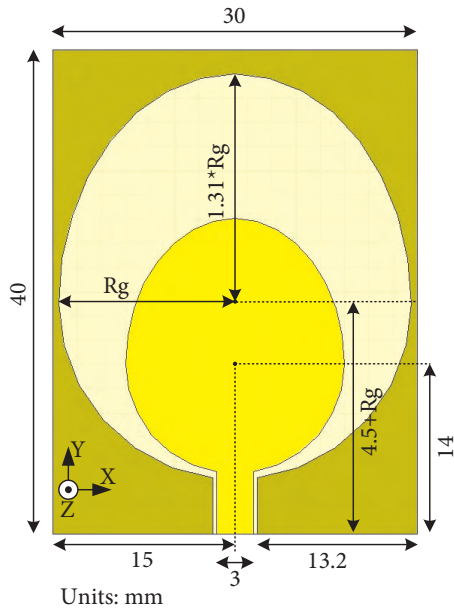


Figure 1. Design with parametrized ground slot.

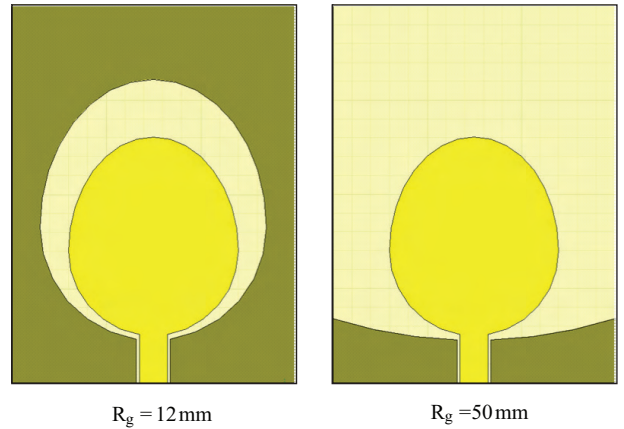


Figure 2. Ground shape for two different  $R_g$  values.

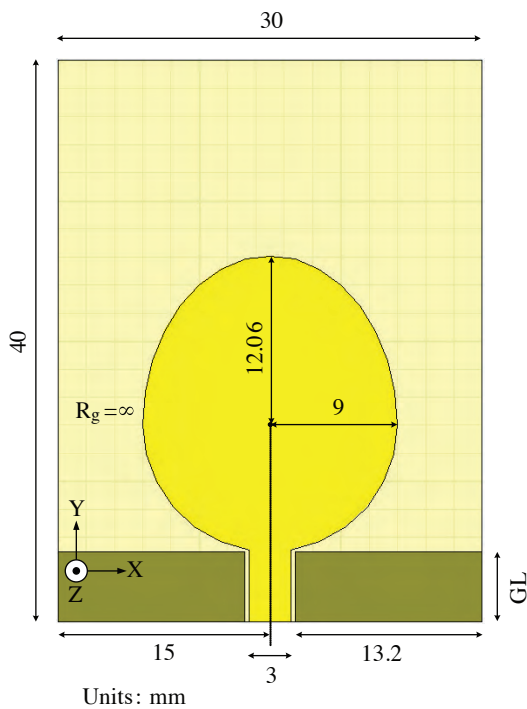


Figure 3. Antenna with partial rectangular ground plane.  $G_L$  to be optimized.

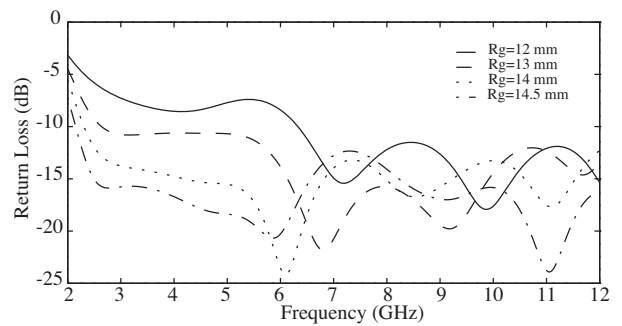
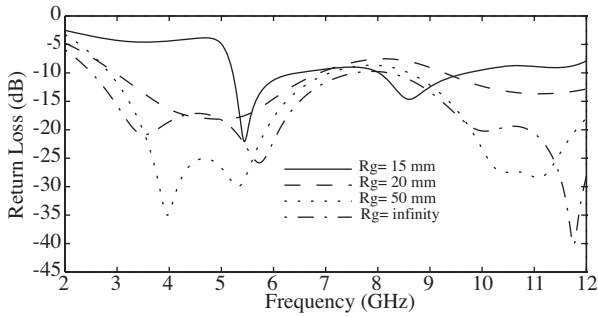
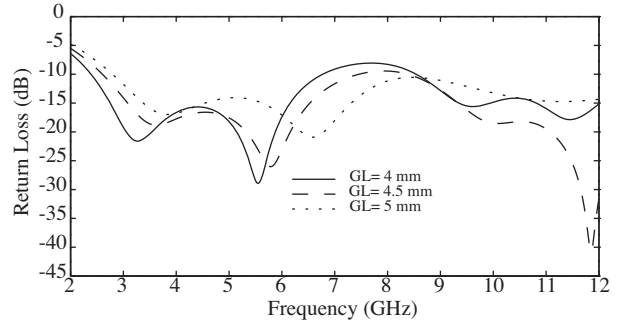


Figure 4. Return loss for some  $R_g$  values. Optimal response for  $R_g = 14.5$  mm.

The plots of Figure 5 show that a UWB response re-emerges as  $R_g \rightarrow \infty$ . The parameter  $G_L$  is optimized to improve the return loss obtained for  $R_g = \infty$ . Figure 6 demonstrates the antenna's return loss as  $G_L$  is varied. A return loss of better than 10 dB over the 2.8–12 GHz frequency range is obtained for  $G_L = 5$  mm. This case is denoted Optimal Design II.



**Figure 5.** Return loss for some  $R_g$  values. UWB response re-emerges for very large  $R_g$ .



**Figure 6.** Return loss for some  $G_L$  values. Good UWB response for  $G_L = 5$  mm.

The HFSS automatic mesher was used in the simulations leading to the results in Figures 4–6. On average, the automatic mesher divided the substrate into about 2800 tetrahedrons, and the radiation box into about 6200 tetrahedrons. Each simulation took around 2 minutes and 35 seconds on a dual-core machine running at 2.2 GHz and having 4 gigabytes of memory.

The two optimal designs, which were reported in [12], are depicted in Figure 7. Their measured and simulated return loss plots are shown in Figures 8 and 9. A good analogy between the measured and computed return loss of both designs is witnessed. One note is that the simulation results in Figures 8 and 9 take into account the thinning of the substrate due to milling effects. This justifies why they are slightly different from their counterparts in Figures 4 and 6.

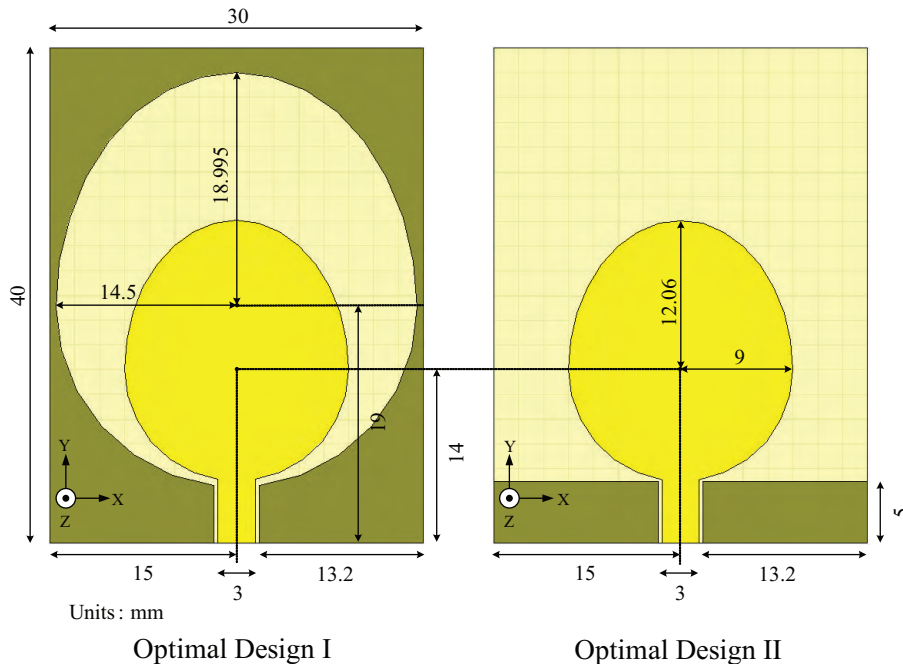


**Figure 7.** Configuration of Optimal Design I (left) and Optimal Design II (right).

The computed peak gain of the two optimal designs is shown in Figure 10. Optimal Design I has an almost flat gain in the 6–12 GHz range, with an average of about 5 dB. Compared to Optimal Design II, it yields higher peak gain values for frequencies up to 7 GHz, but smaller ones beyond that. This is due to the fact that Optimal Design II loses its omni-directional radiation property at high frequencies, which leads to higher and increasing peak gain values.

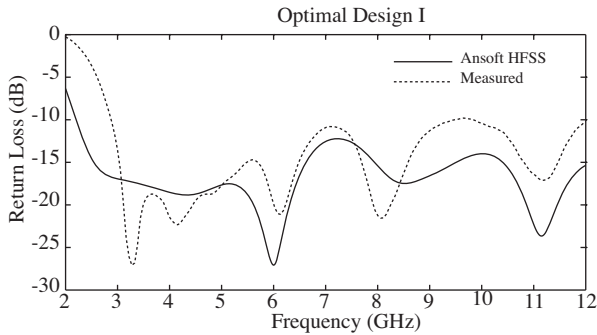


**Figure 8.** Measured and simulated return loss of Optimal Design I.

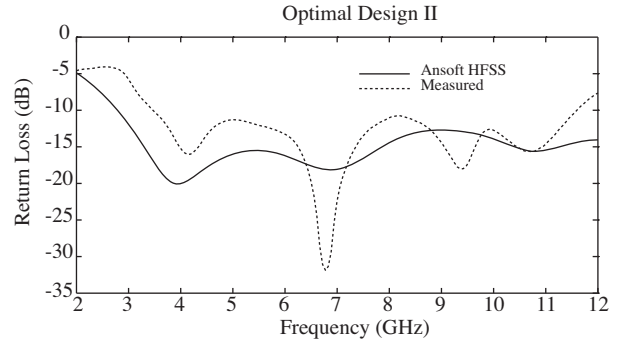


**Figure 9.** Measured and simulated return loss of Optimal Design II.

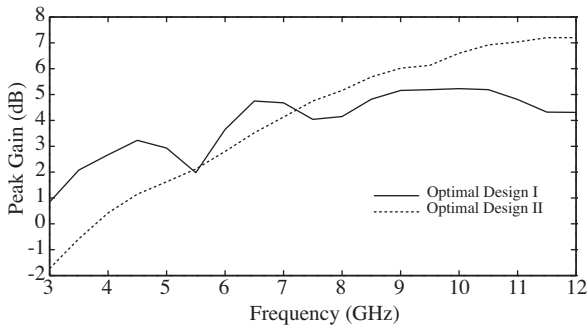


**Figure 10.** Peak gain of the two optimal designs.

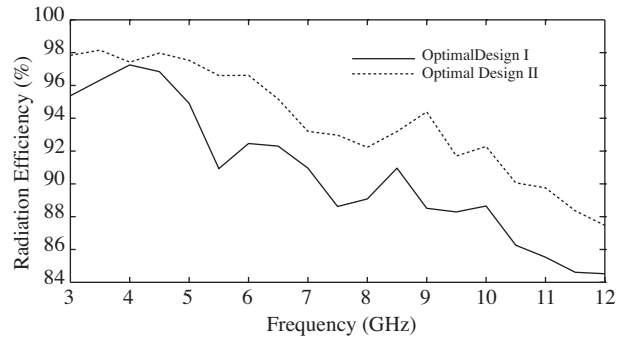


**Figure 11.** Radiation efficiency of the two designs.

Figure 11 shows the radiation efficiency of the two designs. For both, the efficiency decays with increasing frequencies due to more losses in the substrate. Optimal Design II has a slightly larger efficiency.

The computed radiation patterns are given in Figure 12 for 4, 8, and 12 GHz. For verification, the patterns were measured at 4 GHz, and are shown in Figure 13. At 4 GHz, both designs exhibit omni-directional patterns with equal gain in the H-plane (XZ-plane), and a pattern with the shape of figure 8 in the E-plane (YZ-plane). At this frequency, Optimal Design I has a larger gain in both planes. At 8 GHz, Optimal Design II patterns become directional and side-lobes appear, unlike Optimal Design I, which has more consistent omni-directional patterns. This is also evident at 12 GHz where the pattern of Optimal Design I is still satisfactorily omni-directional. At high frequencies, Optimal Design I offers better gains in the H- and E- planes, although Optimal Design II has higher peak gain values.

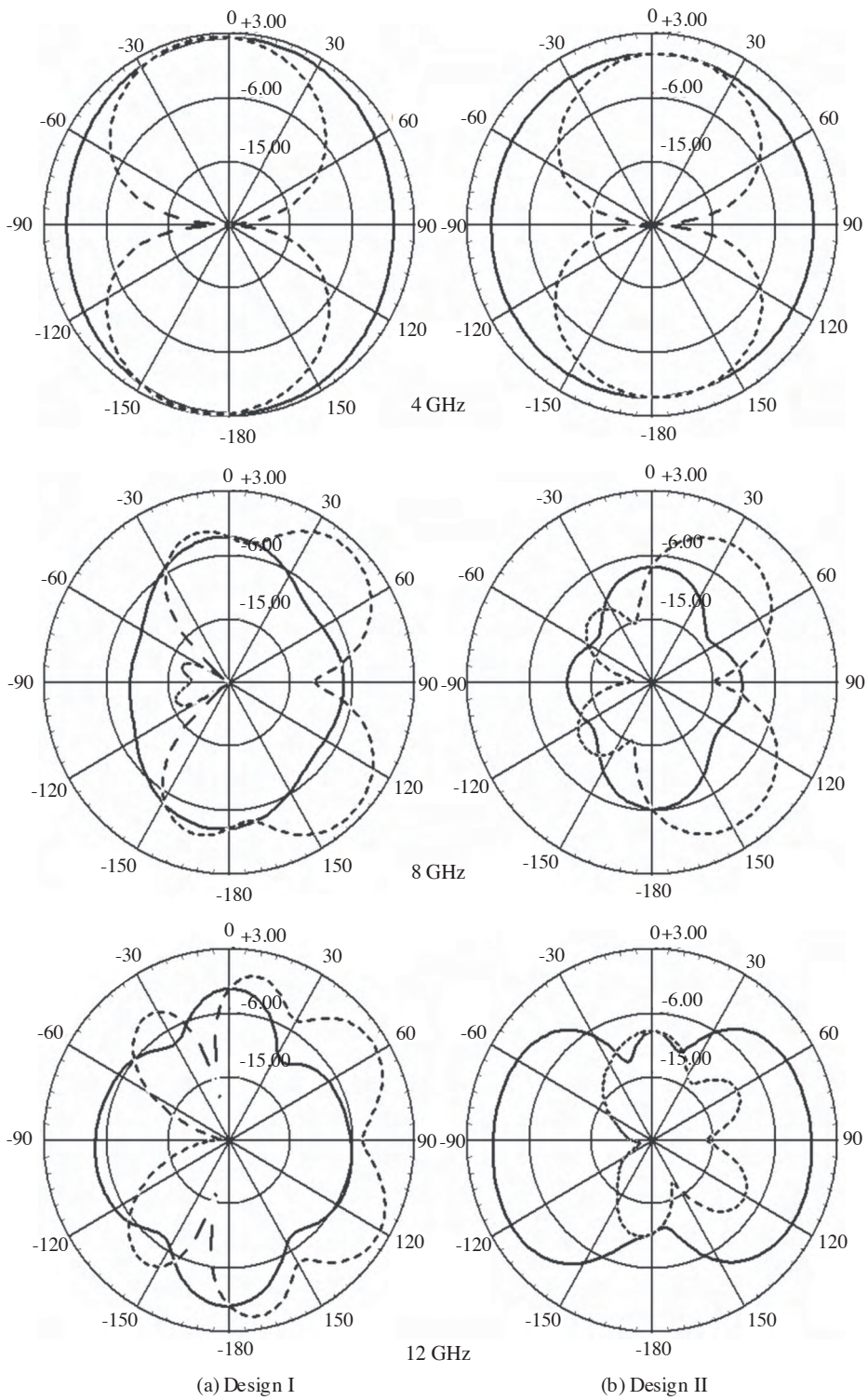


**Figure 12.** Computed radiation patterns of Optimal Design I (left column) and Optimal Design II (right column) in the XZ-plane (solid line) and the YZ-plane (dotted line).



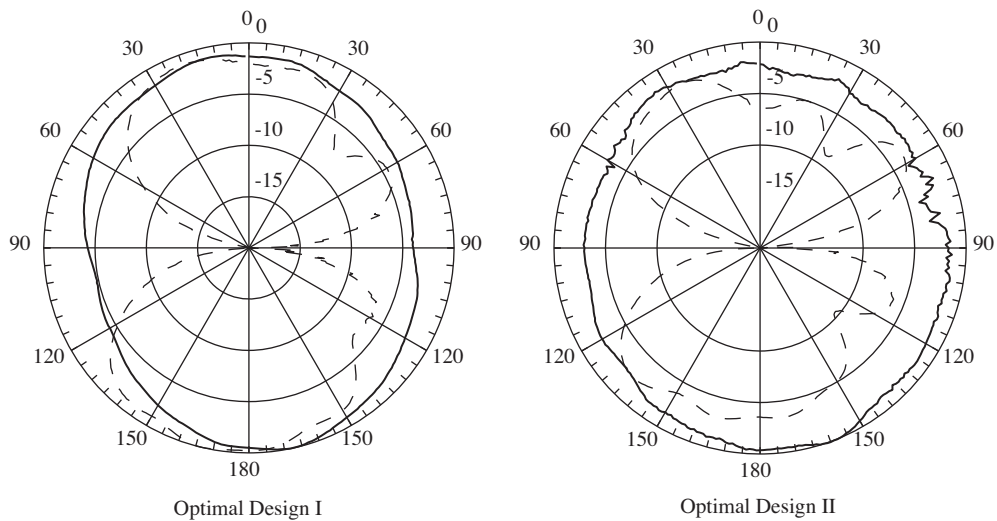


**Figure 13.** Measured radiation patterns of Optimal Design I (left column) and Optimal Design II (right column) in the XZ-plane (solid line) and the YZ-plane (dotted line).

## 4. Conclusion

A printed CPW-fed antenna design for UWB operation was presented. The antenna is based on an FR4 epoxy substrate and an egg-shaped center conductor. A parametric study showed that an egg-shaped slot with  $R_g = 14.5$  mm is optimal in terms of the resulting impedance bandwidth, and that a UWB response re-appears for  $R_g = \infty$ , where the ground plane becomes partial and rectangular in shape. In the latter case, a second parametric study showed that a ground plane length of  $G_L = 5$  mm yields the best return loss response.

Good analogy was witnessed between the measured and computed return loss plots of both optimal designs. Computational results showed that Optimal Design I has better omni-directional radiation properties and higher gain figures in the H- and E- planes. On the other hand, Optimal Design II offered slightly larger radiation efficiencies, and for frequencies larger than 7 GHz, it resulted in higher peak gains.

## Acknowledgement

This work was partially supported by the American University of Beirut Research Board (URB).

## References

- [1] FCC 1st Report and Order on Ultra-Wideband Technology, February 2002.
- [2] C. A. Balanis, *Antenna Theory, Analysis and Design*, Wiley, Hoboken, USA, 2005.
- [3] D.-C. Chang, B.-H. Zeng, J.-C. Liu, "CPW-fed circular fractal slot antenna design for dual-band applications," *IEEE Transactions on Antennas and Propagation*, vol. 56, no. 12, pp. 3630–3636, December 2008.
- [4] A. U. Bhuber, C. L. Holloway, M. Piket-May, R. Hall, "Wide-band slot antennas with CPW feed lines: hybrid and log-periodic designs," *IEEE Transactions on Antennas and Propagation*, vol. 52, no. 10, pp. 2545–2554, October 2004.

- [5] J. Liang, L. Guo, C. C. Chiau, X. Chen, C. G. Parini, "Study of CPW-fed circular disk monopole antenna for ultra-wideband applications," *IEE Proceedings - Microwaves, Antennas and Propagation*, vol. 152, no. 6, pp. 520–526, December 2005.
- [6] J.-Y. Jan, J.-C. Kao, Y.-T. Cheng, W.-S. Chen, H.-M. Chen, "CPW-fed wideband printed planar monopole antenna for ultra-wideband operation," in *The 2006 IEEE AP-S International Symposium and URSI National Radio Science Meeting*, Albuquerque, New Mexico, 9–14 July 2006, pp. 1697–1700.
- [7] M.-E. Chen, J.-H. Wang, "CPW-fed crescent patch antenna for UWB applications," *Electronics Letters*, vol. 44, no. 10, pp. 613–614, May 2008.
- [8] L. Zhao, C.-L. Ruan, S.-W. Qu, "A novel broad-band slot antenna fed by CPW," in *The 2006 IEEE AP-S International Symposium and URSI National Radio Science Meeting*, Albuquerque, New Mexico, 9–14 July 2006, pp. 2583–2586.
- [9] E. S. Angelopoulos, A.Z. Anastopoulos, D.I. Kaklamani, A.A. Alexandridis, F. Lazarakis, and K. Dangakis, "Circular and elliptical CPW-fed slot and microstrip-fed antennas for ultrawideband applications," *IEEE Antennas and Wireless Propagation Letters*, vol. 5, pp. 294–297, 2006.
- [10] P. Li, J. Liang, and X. Chen, "Study of printed elliptical/circular slot antennas for ultrawideband applications," *IEEE Transactions on Antennas and Propagation*, vol. 54, no. 6, pp. 1670–1675, June 2006.
- [11] Ansoft HFSS, Pittsburgh, PA 15219, USA.
- [12] M. Al-Husseini, A. Ramadan, Y. Tawk, A. El-Hajj, K. Y. Kabalan, "Design and ground plane consideration of a CPW-fed UWB antenna," in *The 2009 International Conference on Electrical and Electronics Engineering*, Turkey, Bursa, 5–8 November 2009, pp. II-151–II-153.